

DFTT 52/97
August 1997

Six fermion processes at future e^+e^- colliders: signal and irreducible background for top, WWZ and Higgs physics in charged current final states.¹

Elena Accomando, Alessandro Ballestrero and Marco Pizzio

*I.N.F.N., Sezione di Torino, Italy
and*

*Dipartimento di Fisica Teorica, Università di Torino, Italy
v. Giuria 1, 10125 Torino, Italy.*

Abstract

We compute several total and differential cross sections relevant to top, WWZ and Higgs physics at future e^+e^- colliders taking into account the full set of Feynman diagrams for six fermion final states. We examine in particular charged current processes, in which final particles cannot be formed by three Z's decay. We include in our calculations initial state radiation and beamstrahlung effects, and the most important QCD corrections in an approximate (naive) form. We also compare this complete approach with *production* \times *decay* approximation.

Contribution to the Proceedings of the "ECFA/DESY Study on Physics and Detectors for the Linear Collider", February to November 1996, ed. R. Settles, Desy 97-123E.

¹ Work supported in part by Ministero dell' Università e della Ricerca Scientifica.

e-mail: accomando,ballestrero,pizzio@to.infn.it

1 Introduction

Processes with many particles in the final state become more and more important at high energies for present and future accelerators. At LEP2 WW and Higgs physics has lead to a careful study of all complete four fermion final states, for which electroweak dedicated codes have been constructed (for a review on the argument see [1][2][3]). When future e^+e^- colliders will come into operation, states with even more final particles will become important. In particular all physics regarding top studies, three vector boson production and intermediate Higgs searches will deal with six fermion final states.

The complete calculation of such processes is rather complicated even at tree level: it requires the computation of hundreds of Feynman diagrams. The alternative is that of considering only the most important contributions to them, which generally correspond to diagrams in which unstable particles (W, Z, top, Higgs) can go on mass shell, and evaluate them in the *production* \times *decay* approximation. With such a method it is also easier to compute the most important higher order corrections. On the other hand one is neglecting the contributions of a lot of diagrams, interference effects, spin correlations effects, off-shellness of the resonant diagrams, and only the complete calculation can establish case by case the reliability of such approximations, which often depends on final states, cuts, energies and distributions.

All processes $e^+e^- \rightarrow$ *six fermions* can be divided according to their final states. As for four fermion final states, we can identify Charged Currents (CC), Neutral Currents (NC) and Mixed processes (MIX) [4][2][3]. We call CC the six fermion processes in which the final particles can form two W's and a Z but not three Z's (e. g. $\mu\bar{\nu}u\bar{d}e^+e^-$), NC those in which three Z's and not two W's and a Z can be formed (e. g. $u\bar{u}\mu^+\mu^-e^+e^-$), MIX those in which both can be formed (e. g. $u\bar{u}d\bar{d}e^+e^-$).

As already mentioned, these reactions are of particular interest because they are related to top, WWZ and Higgs physics. If we consider for instance a final state like $b\bar{b}\mu\bar{\nu}_\mu u\bar{d}$, this may be produced by the decay of WWZ or come from two W's and two b's, which in turn may descend from two tops. WWZ intermediate state may be due to Higgs-Z production with an Higgs decaying into two W's. Of course the various channels are not separated in the reality, and many more diagrams (irreducible background) contribute to such processes. They can be distinguished only for their different contribution to various zones of the phase space and can eventually be disentangled by applying experimental cuts. In order to study such cuts, and to evaluate the magnitude of the various contributions after they have been applied, one must use the full calculation.

We have produced a code (SIXPHACT) to compute all six fermions CC processes. With it we will examine top top in the continuum, WWZ and intermediate Higgs events. In all three cases the signal intermediate state contains two W's. We will in particular discuss those processes in which (at least) one isolated lepton (e.g. a μ^- without the corresponding μ^+) indicates the presence of two W's. A part of this analysis has already been reported in ref [5] to which we refer for details. Top and Higgs physics have already been analyzed within a four particles ($b\bar{b}W^+W^-$) final state approximation [6]. Six fermion physics has also been considered in [7][8]. In particular in ref.[7] the processes $e^+e^- \rightarrow \mu^+\mu^-\tau^-\bar{\nu}_\tau u\bar{d}$ and $e^+e^- \rightarrow \mu^+\mu^-e^-\bar{\nu}_e u\bar{d}$ have been analyzed for their

interest in Higgs searches, while ref.[8] deals with the reaction $e^+e^- \rightarrow b\bar{b}u\bar{d}\mu^-\bar{\nu}_\mu$ and its relation to top physics.

To give an idea of the complexity of the problem, we remind that the process $e^+e^- \rightarrow b\bar{b}u\bar{d}\mu^-\bar{\nu}_\mu$ has 232 tree level diagrams, $e^+e^- \rightarrow e^-\bar{\nu}_e u\bar{d}s\bar{s}$ 420, and $e^+e^- \rightarrow e^-\bar{\nu}_e u\bar{d}e^-e^+$ 1254. The integration variables are at least thirteen, but they become seventeen for the more realistic case in which initial state radiation (ISR) and beamstrahlung (BST) are accounted for. For such reasons it is extremely important to use a method for computing helicity amplitudes which allows a very fast and precise computation. We have used to this end PHACT [9], a set of routines based on the method of ref.[10], in order to generate the fortran code for the amplitudes. We have computed all Feynman diagrams by calculating subdiagrams of increasing complexity and reusing them whenever needed. The method used is particularly suited for this procedure. We have introduced ISR via the structure function method [11] and BST with a link to the program CIRCE [12]. Different phase spaces with different mappings to account for various peak structures have been employed. The numerical integration has been performed with VEGAS[13].

As far as QCD corrections are concerned, we have introduced them in the so called naive QCD approach (NQCD). This amounts to consider that we have diagrams with vertices which in narrow width approximation (NWA) correspond to *production* \times *decay* of W's, Z's, t's, h's. The corresponding corrections for the decay are factorized and we multiply such diagrams for these factors. We have also included QCD corrections in the naive formulation to the $t\bar{t}$ production vertices. The first order QCD corrections [14] to σ_{VV} and σ_{AA} , the vector-vector and axial-axial contributions to the total on-shell top top cross section, factorize separately. We have introduced these corrections, but we have not applied any correction to the interference term σ_{VA} which vanishes when integrated over the full phase space. Our treatment of QCD corrections is in any case exact only in the narrow width approximation for the total cross section with no cuts. In all other cases it must be considered as a rough estimate of the most important QCD corrections. In many cases this has however proved to be a reasonable approximation, probably just because the error on the corrections reflects upon a much smaller error on the cross sections.

For the numerical part we have used the G_μ -scheme

$$s_w^2 = 1 - \frac{M_w^2}{M_z^2}, \quad g^2 = 4\sqrt{2}G_\mu M_w^2 \quad (1)$$

and the input masses $m_Z = 91.1888$ GeV, $m_W = 80.23$ GeV. We have chosen $m_t = 180$ GeV and for m_b the running mass value $m_b = 2.7$ GeV. For the strong corrections to Z, W top and Higgs decay widths and vertices we have used $\alpha_s(m_Z) = 0.123$ and evolved it to the appropriate scales.

We have moreover implemented the following general set of cuts :

$$\begin{aligned} \text{jet(quark) energy} &> 3 \text{ GeV}; & \text{lepton energy} &> 1 \text{ GeV}; & \text{jet-jet mass} &> 10 \text{ GeV}; \\ \text{lepton-beam angle} &> 10^\circ; & \text{jet-beam angle} &> 5^\circ; & \text{lepton-jet angle} &> 5^\circ. \end{aligned}$$

Other cuts specific to particular studies will be described in the following.

2 Top in the continuum

After top discovery and the measurement of its mass ($m_t = 174 \pm 6$ GeV) [15], its properties must be determined with high-precision. An extremely important characteristic of the top is its lifetime, which is much shorter than the time scale of strong interactions, allowing to study it in the context of perturbative QCD. The opening of a new channel and perturbative effects [16] determine a sharp rise of the cross section at threshold. For such a reason, the best strategy to measure top mass at future e^+e^- colliders consists in running at $t\bar{t}$ threshold, while its static properties, such as magnetic and electric dipole moments [17] will be measured with high accuracy in the continuum, at higher energies. In any case, future e^+e^- colliders will produce a great number of top top events: at 500 GeV the cross section $\sigma(t\bar{t})$ is of the order of .5 pb, which corresponds to about 2.5×10^4 events for an integrated luminosity of 50 fb^{-1} .

The results in the following refer only to the continuum top top production. The tree level matrix elements for the complete calculation of the various final states do not take into account the above mentioned threshold corrections. They can nevertheless be useful to estimate the relevance of the irreducible background due to all non double resonant diagrams also at threshold.

We will consider two specific CC final states: $e^+e^- \rightarrow \mu\bar{\nu}_\mu u\bar{d}b\bar{b}$ and $e^+e^- \rightarrow e\bar{\nu}_e u\bar{d}b\bar{b}$. The cross sections due to signal diagrams only, and the irreducible backgrounds due to all other diagrams (207 for the μ and 416 for the e without Higgs) and their interference with the signal at 500 and 800 GeV are given in table 1. Here and in the following

\sqrt{s} GeV	channel	$t\bar{t}$ signal (fb)	background (fb)
500	$\mu\bar{\nu}_\mu u\bar{d}b\bar{b}$	19.850(4)	0.736(3)
	$e\bar{\nu}_e u\bar{d}b\bar{b}$		0.778(5)
800	$\mu\bar{\nu}_\mu u\bar{d}b\bar{b}$	10.700(2)	1.007(4)
	$e\bar{\nu}_e u\bar{d}b\bar{b}$		1.21(2)

Table 1: Cross section for the processes $e^+e^- \rightarrow \mu\bar{\nu}_\mu u\bar{d}b\bar{b}$ and $e^+e^- \rightarrow e\bar{\nu}_e u\bar{d}b\bar{b}$.

we report between parenthesis the statistical integration errors on the last digit of the result.

These values have been obtained taking into account b masses, the full set of diagrams (without Higgs), ISR, BST, NQCD corrections for the decay vertices of the W's, the Z, tops and also for Z(γ)tt vertex, as already explained.

In table 2 we report the cross sections for $e^+e^- \rightarrow \mu\bar{\nu}_\mu u\bar{d}b\bar{b}$ for different approximations, in order to understand the relevance of these corrections. The first result (NWA) reproduces what one would obtain using on shell calculation of $t\bar{t}$ production with subsequent decays of the tops to bW and on shell decay of the W's. The second result corresponds to the Born approximation, to which we add in the following ones ISR, naive QCD corrections to t's, W's and Z decay vertices (NQCD*), these plus that of Z(γ)tt vertex (NQCD), beamstrahlung for the TESLA parametrization (BST) and

$e^+e^- \rightarrow \mu\bar{\nu}u\bar{d}b\bar{b}$	$t\bar{t}$ signal (fb)	background (fb)
NWA	18.880(3)	0.848(3)
Born	18.286(3)	0.824(3)
ISR	17.419(3)	0.750(3)
ISR NQCD*	17.188(3)	0.753(3)
ISR NQCD* BST	17.303(3)	0.731(3)
ISR NQCD* SBAND	17.308(3)	0.728(3)
ISR NQCD* BST m_b	17.352(3)	0.736(3)
ISR NQCD BST m_b	19.850(4)	0.736(3)

Table 2: Cross section for the process $e^+e^- \rightarrow \mu\bar{\nu}u\bar{d}b\bar{b}$ at $\sqrt{s} = 500$ GeV for different sets of approximations

for the SBAND one. The results of the last two lines have been obtained taking exactly into account the mass (m_b) of the b 's, which were considered massless in the previous ones in table 2.

Let us now consider the irreducible background due to all diagrams contributing to a final state. From table 1 one can conclude that the background represents a correction of about 4% to the signal. It is however important to understand, with the help of figs. 1 and 2, where this difference manifests itself in the distributions.

In fig. 1 it is reported the invariant mass distribution of the top candidate in the channel $e^+e^- \rightarrow \mu\bar{\nu}u\bar{d}b\bar{b}$. The differential cross sections for $e^+e^- \rightarrow e\bar{\nu}u\bar{d}b\bar{b}$ are practically identical. From table 1 one can easily see in fact that the difference between the two channels (μ and e) is sizeable with respect to the backgrounds themselves, but it amounts to only a few permill of the signal.

For a process of this kind, one should try to identify the particles which might come from a top decay, in order to measure their invariant mass. It is experimentally difficult to reconstruct the invariant mass of the muon, its neutrino and \bar{b} , as the neutrino momentum can only be deduced from missing momentum, to which also ISR and BST contribute. It is probably better to look for the three quarks forming the top. We assume that there is b tagging, and we require that both b 's are identified, so that they are separated from the other two quarks. One cannot distinguish between a b and a \bar{b} , therefore one measures both the two invariant masses formed with one of the two b 's and the two other light quarks. Considering both values for every event, one obtains a distribution with which it will be possible to measure the mass of the top. Once this has been measured, one can refine the sample and look event by event for the nearest to the expected top mass between the two. We refer to this one as the mass of the top candidate, and we have plotted its distribution. In fig. 1 one can see the differences among this distribution for the full process, the one due to the signal diagrams and that obtained with only background diagrams. This last distribution too

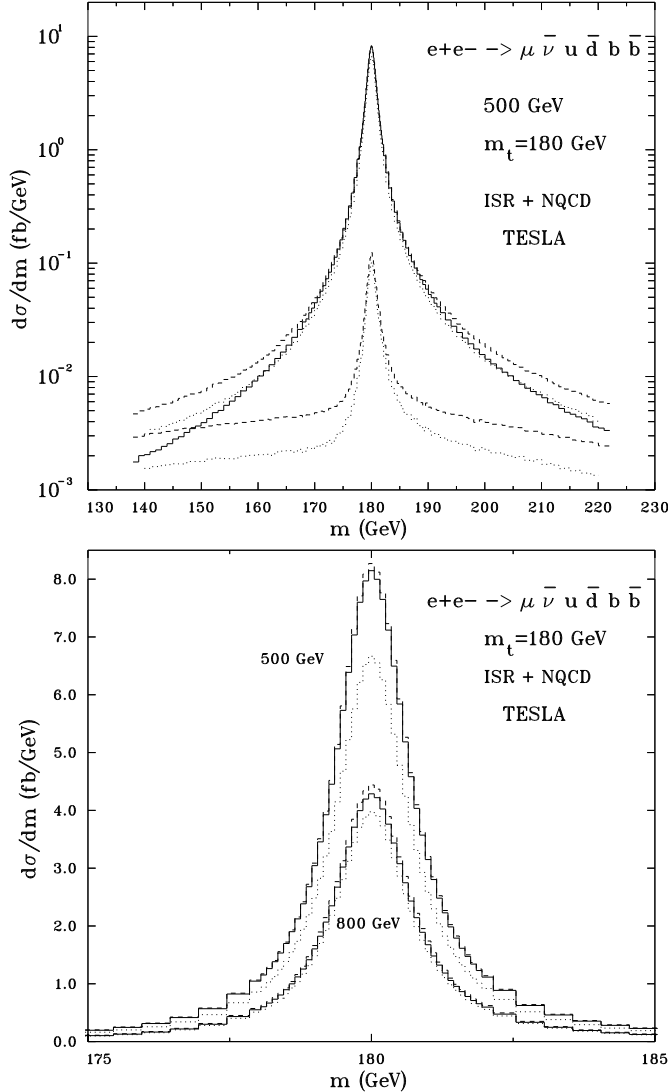


Figure 1: Invariant mass distributions for top candidate. The nearest to the nominal top mass between $u\bar{d}b$ or $u\bar{d}\bar{b}$ invariant masses is chosen event by event. In the upper part the two lower curves represent the irreducible background with and without cuts described in the text. All other lines represent the contribution of $t\bar{t}$ off shell signal (solid), the full process (dash) and the full process after cuts (dot).

peaks at the top mass. This is of course the effect of the many diagrams which are "single resonant", in which one of the two top propagators can go on mass shell. We have also computed the same distribution after some cuts have been applied in order to try to eliminate the background (dotted lines). The cuts we have imposed are:

$$|m(u\bar{d}) - m_W| < 20 \text{ GeV} \quad |m(b\bar{b}) - m_Z| > 20 \text{ GeV} \quad (2)$$

One can see that these cuts reduce in fact the background by about a factor two, but they do not affect its peak at the top mass.

In the lower part of fig. 1 we have reported on a linear scale and on the neighborhood of the peak the three curves relative to full process, signal and full process after cuts, both at 500 GeV and at 800 GeV. From these curves one concludes that there does not seem to be any difference in the location of the maximum, but there are some appreciable differences in the height between signal and total distributions. The cuts (2) are practically useless in this region.

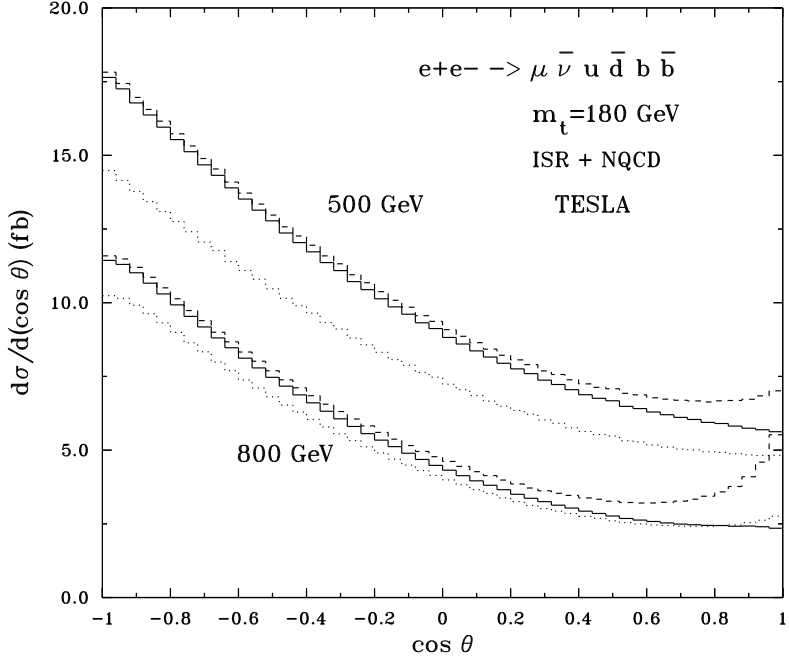


Figure 2: Angular distribution for top candidate at $\sqrt{s} = 500$ GeV (upper) and $\sqrt{s} = 800$ GeV (lower). The solid lines represent the contribution of $t\bar{t}$ off shell signal, the dash lines the full process and the dot lines the full process after cuts.

We have also studied the angular dependence of the top candidate. If one compares the dashed and full curves of fig. 2, one notices that both at 500 GeV and at 800 GeV, there is a difference in the angular distribution between signal and total calculations. This is particularly relevant in the forward e^+ direction. The contribution of the irreducible background, may be reduced if one imposes the cuts (2) and a cut on the mass of the top candidate m_{tc} :

$$|m_{tc} - m_t| < 40 \text{ GeV} \quad (3)$$

As it can be seen from the dotted curves, there remains however a mild distortion of the total curve with respect to the signal one, also after the cuts.

3 WWZ and its background

The main interest in WWZ production lies in the possibility to measure gauge couplings. In particular the quartic gauge coupling and its possible deviations from SM will be studied at future e^+e^- colliders. Several authors [18, 19] have already analyzed three vector boson production and anomalous gauge couplings. LHC measurements on VV+X (V=W,Z) final states will probably reach a better quartic gauge sensitivity than the WWZ measurement at 500 GeV e^+e^- colliders.[20, 19], nevertheless a careful six fermion study of triple boson production is needed. In particular the possible background from $t\bar{t}$ production or top resonant diagrams may be dangerous and has to be analyzed in detail. We consider in this section WWZ signal and its irreducible backgrounds in the channels with four quarks and an isolated lepton. Among these, discriminating with b -tagging those final states not containing b quarks can help to reduce most of $t\bar{t}$ background.

The diagrams one has to deal with are similar to those of the preceding section. The total cross section is however lower by an amount comparable to $t\bar{t}$ production as this type of diagram is now no more resonant when there are no final b's. The most important contribution comes from the 15 diagrams which correspond to WWZ production and decay. We will call them signal diagrams. The remaining ones can be divided in double, single and non resonant parts.

The results we will present take into account ISR, BST, NQCD.

In table 3 we present the cross sections for the full processes, those computed taking into account signal diagrams only, and those computed via the *production* \times *decay* approximation. This last result has been obtained taking the narrow width approximation limit of the signal diagrams.

process	WWZ NWA (fb)	WWZ signal (fb)	complete (fb)
$\mu\bar{\nu}ud\bar{c}\bar{c}$	0.13836(2)	0.13464(2)	0.16218(9)
$e\bar{\nu}ud\bar{c}\bar{c}$			0.1783(2)
$\mu\bar{\nu}ud\bar{s}\bar{s}$	0.17780(3)	0.17303(3)	0.1803(1)
$e\bar{\nu}ud\bar{s}\bar{s}$			0.2117(2)
$\mu\bar{\nu}u\bar{d}u\bar{u}$	0.12815(2)	0.12469(2)	0.1512(1)
$e\bar{\nu}u\bar{d}u\bar{u}$			0.1758(3)
$\mu\bar{\nu}u\bar{d}d\bar{d}$	0.16468(3)	0.16025(3)	0.16733(9)
$e\bar{\nu}u\bar{d}d\bar{d}$			0.1941(1)

Table 3: Cross section for the processes $e^+e^- \rightarrow l\bar{\nu}_l + 4$ light quarks ($l = \mu, e$) at $\sqrt{s} = 500$ GeV

The difference between the full calculation and on shell (NWA) approximation is indeed remarkable. Even between signal and NWA there is a variation of some percent. The background is much higher in a process with an up-type quark pair than in the analogous one with down-type. For instance $\mu\bar{\nu}ud\bar{c}\bar{c}$ background is .0275fb while the $\mu\bar{\nu}ud\bar{s}\bar{s}$ is .0073fb. This corresponds to the fact that, for the set of cuts we are using, most background comes from diagrams with two resonant W's and a γ converting in a quark-antiquark pair. Diagrams with one resonant W and the pair coming from Z decay would in fact produce an opposite behaviour.

In presence of such big irreducible background, it is necessary to introduce cuts in order to try to isolate WWZ production. We have implemented in figs. 3,4 and 5 different cuts on invariant masses of the pairs of particles which should come from vector bosons, and computed the cross sections with the full set of diagrams (continuous line), with only the fifteen signal diagrams (dashed), and with *production* \times *decay* or narrow width approximation (dotted). Obviously these last cross sections are not sensible to such kind of cuts. We consider at first some cuts which act only on the quarks, as the neutrino momentum is not directly measurable. We accept an event if out of the three

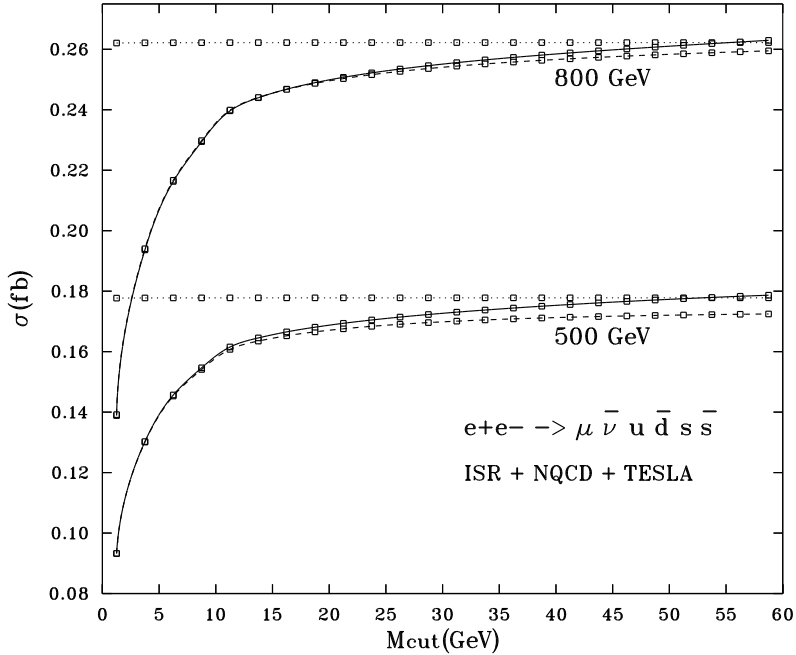


Figure 3: Cross section for the process $e^+e^- \rightarrow \mu\nu_\mu u\bar{d}s\bar{s}$ as a function of M_{cut} at $\sqrt{s} = 500$ GeV (lower) and $\sqrt{s} = 800$ GeV (upper). Quarks are required to form two pairs whose invariant masses m_i ($i = 1, 2$) satisfy the conditions $|M_V - m_i| < M_{cut}$, $V = W, Z$. The dot lines represent the cross section due to WWZ on shell, the dashed ones the contribution of resonant WWZ diagrams only, the continuous the complete cross section. The markers indicate the points effectively computed.

couple of pairs of quarks, one at least has a pair whose invariant mass m_1 satisfies $|M_W - m_1| < M_{cut}$ and the other pair's mass m_2 satisfies $|M_Z - m_2| < M_{cut}$. In figs. 3-4 are reported the corresponding cross sections as a function of M_{cut} . Both figures show that the signal contribution to the cross section is lower than the NWA even for very loose cuts or for the cross section without cuts (see table 3). The curves of fig. 4 show that for the electron case the difference between signal and total process is extremely relevant. It grows with the energy and the cuts we have imposed can greatly reduce the difference but not suppress it. For the muon case an M_{cut} of about 10 GeV is on the contrary sufficient to make total and signal cross section practically coincide. The loss in event number is however of the order of ten percent. In order to further suppress the background in the electron case, we have also imposed a cut on the invariant mass M_{rec} formed with the four momentum of the electron and the reconstructed neutrino one. In such a case we attribute all missing three-momentum \bar{p}_{mis} to the neutrino and take its energy to be equal to $|\bar{p}_{mis}|$. We have indeed verified that even a very loose cut as $|M_W - M_{rec}| < 60$ GeV reduces significantly the difference between signal and total cross sections. On the other hand, if the cut has to be so stringent as to reduce the difference between signal and total cross section to the order of the percent, i.e. $|M_W - M_{rec}| < 15$ GeV, one loses about one third of the event number, as compared to the NWA. This conclusion is important in view of the fact that such WWZ processes have a low cross section: at 500 GeV $\sigma(\text{WWZ})$ is of the order of 40 fb, which corresponds to a total of 2000 events for an integrated luminosity of 50 fb^{-1} .

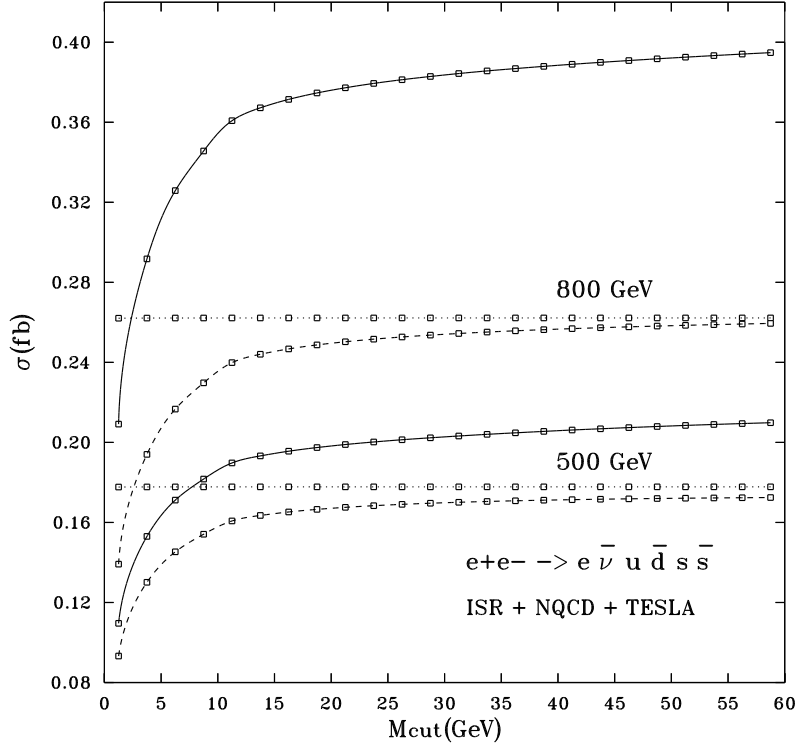


Figure 4: Cross section for the process $e^+e^- \rightarrow e^-\bar{\nu}_e u\bar{d}s\bar{s}$ at $\sqrt{s} = 500$ GeV (lower) and $\sqrt{s} = 800$ GeV (upper) as a function of M_{cut} . The definition of M_{cut} and the meaning of the different lines and of the markers is the same as in fig 3.

The reactions studied in figs. 3-4 cannot be directly measured, as the different quark flavours cannot be disentangled experimentally. In fig. 5 we examine the more interesting physical case in which we sum over all reactions involving one isolated muon. In the plot it is reported, both for WWZ diagrams and for the complete calculation, the sum of the cross sections for

$$e^+e^- \rightarrow \mu^-\bar{\nu}_\mu u\bar{d}s\bar{s} \quad e^+e^- \rightarrow \mu^-\bar{\nu}_\mu u\bar{d}c\bar{c} \quad e^+e^- \rightarrow \mu^-\bar{\nu}_\mu u\bar{d}u\bar{u} \quad e^+e^- \rightarrow \mu^-\bar{\nu}_\mu u\bar{d}d\bar{d}$$

multiplied by a factor 4. This accounts for the reactions in which one has $\mu^+\nu_\mu\bar{u}d$ instead of $\mu^-\bar{\nu}_\mu u\bar{d}$ and for those in which one has $c\bar{s}$ (or $\bar{c}s$) instead of $u\bar{d}$ (or $\bar{u}d$). The dashed and continuous lines of fig. 5 give therefore the total cross section as a function of M_{cut} for all processes with one muon, four quarks and no b's in the final state.

In order to reduce the enormous background from $t\bar{t}$ production and decay, b-tagging will be used. With it, one can exclude all events with at least one tagged b. With actual b-tagging techniques, this however leads to a reduction of the signal without completely suppressing the background. In fact, if there is a high probability $P_{c \rightarrow b}$ that a c be misidentified as a b, one has to multiply by the appropriate reduction factors $1 - P_{c \rightarrow b}$, $(1 - P_{c \rightarrow b})^2$, $(1 - P_{c \rightarrow b})^3$ the contributions with one, two or three c's to the the above sums. This would give a decrease of the signal curves of about 25% for $P_{c \rightarrow b} = .3$. Moreover if there is a finite probability $P_{b \neq b} = 1 - P_{b \rightarrow b}$ that a b may not be recognized as such, events with two b's can be misidentified and give a residual background to WWZ physics. The chain dash and chain dot curves of fig. 5 correspond to such a background as a function of M_{cut} . We have assumed $P_{b \neq b} = .2$ and summed over the processes

$$e^+e^- \rightarrow \mu^-\bar{\nu}_\mu u\bar{d}b\bar{b} \quad e^+e^- \rightarrow \mu^-\bar{\nu}_\mu c\bar{s}b\bar{b} \quad e^+e^- \rightarrow \mu^+\nu_\mu u\bar{d}b\bar{b} \quad e^+e^- \rightarrow \mu^+\nu_\mu c\bar{s}b\bar{b}.$$

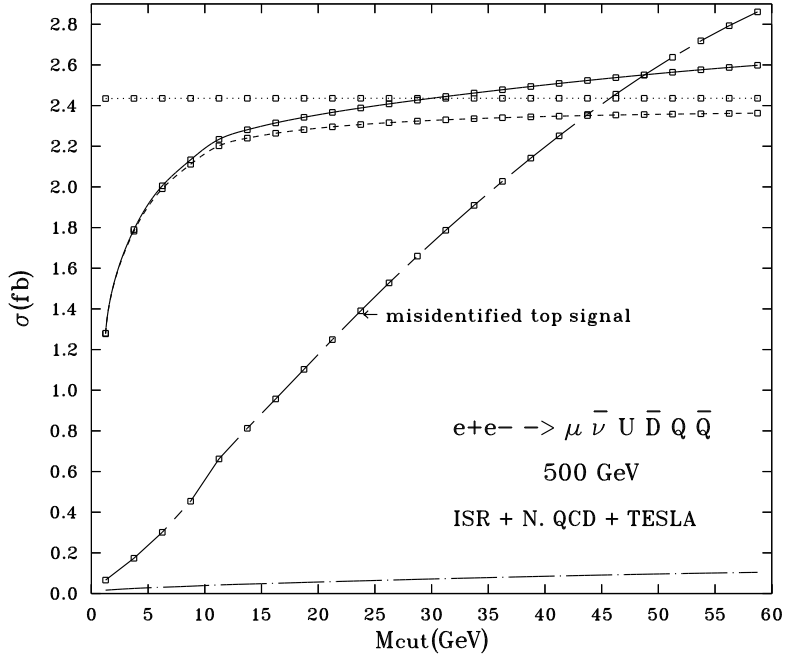


Figure 5: cross section for $e^+e^- \rightarrow \mu\nu UD\bar{Q}\bar{Q}$ as a function of M_{cut} . We sum over all processes with one muon and no b quarks. The chaindash (chaindot) line represents the background due to top top signal (background) with both misidentified b's. The definition of M_{cut} and the meaning of the different lines and of the markers is the same as in fig 3.

From these curves, one can conclude that even an imperfect b tagging is of considerable help in strongly reducing the great number of these events. It has to be remarked that this background depends strongly on the applied M_{cut} . If one adopts the strategy of applying a severe M_{cut} of the order of 10 GeV, it is reduced to about 1/6 of WWZ signal. If on the other hand a milder M_{cut} is used or if $P_{b \not\rightarrow b}$ is greater than what we used, it may become comparable to the signal itself.

4 Intermediate mass Higgs.

We will consider in this section the scenario in which the Higgs mass is in the intermediate range. As it is well known a light Higgs decays predominantly to $b\bar{b}$ pairs. When the mass of the Higgs is of the order of 140 GeV, $b\bar{b}$ and WW^* decays become comparable. After the threshold for two W's production, W^+W^- decay becomes the dominant one, its branching being almost one at threshold and of the order of .7 for higher masses, where two Z's decay is kinematically allowed. As far as production of the Higgs is concerned, the dominant process at e^+e^- is HZ production (Higgs bremsstrahlung) up to a c.m. energy of 500 GeV, where the WW fusion process has about the same magnitude as the previous one. At higher energies this last process dominates.

Most Higgs events will in effect appear as six fermion events for a mass above 140 GeV. Those coming from WW fusion will be characterized by two neutrinos and four fermions coming from the chain decay $H \rightarrow W^+W^- \rightarrow 4f$. If one of the W's decays leptonically, there will be at least three neutrinos around, and it will be difficult to

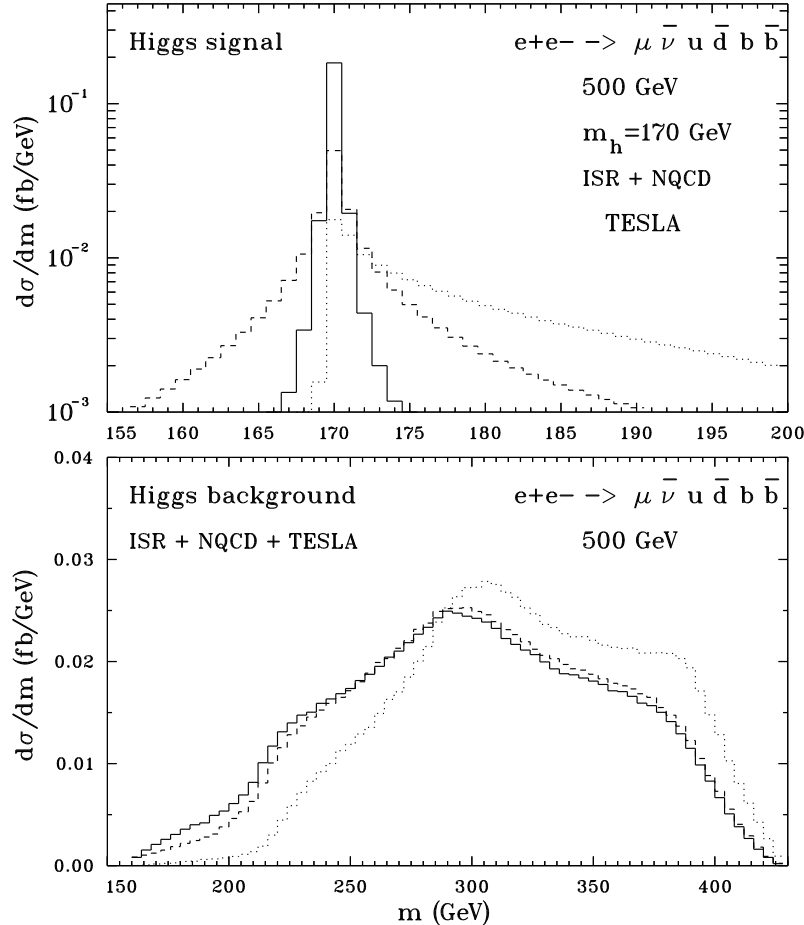


Figure 6: Invariant mass distributions for Higgs signal (upper) and background (lower). The continuous line corresponds to $(\mu \bar{\nu} u \bar{d})$ mass, the dashed to the *reconstructed* and the dot to the *missing* one.

reconstruct the Higgs invariant mass. Therefore WW fusion events will be mainly studied in 4q + 2*ν*'s final state. This implies that six fermion background to these events will come from NC, MIX and CC processes and it will be rather complicated to deal with.

We limit our present analysis to CC processes. We examine therefore in some detail Higgs bremsstrahlung for an intermediate mass Higgs in the following final states:

$$1) l \nu_l + 4 q's, \quad 2) l \nu_l + l' \bar{l}' + 2 q's, \quad 3) l \nu_l + l' \nu_{l'} + 2 q's.$$

Typical examples are respectively $e^+e^- \rightarrow \mu \bar{\nu} u \bar{d} b \bar{b}$, $e^+e^- \rightarrow e \bar{\nu} u \bar{d} \mu^+ \mu^-$, $e^+e^- \rightarrow \mu \bar{\nu}_\mu e^+ \nu_e s \bar{s}$. Considering the branching of the W's and of the Z, one can deduce that the percentage of all processes of type 1) with respect to the full HZ signal is about 31%. The others are approximately 4.4% for 2) and 5.2% for 3). These values have been obtained including also the τ 's. In case 3) we have not taken into account the decays in which l and l' have the same flavour. Let us recall that at a center of mass energy of 500 GeV one has a cross section for $e^+e^- \rightarrow HZ$ of approximately 40 fb for an Higgs mass of the order of 200 GeV. For an integrated luminosity of 50 fb^{-1} per year, this means around 2000 HZ events and about 600 events for case 1), 100 each for

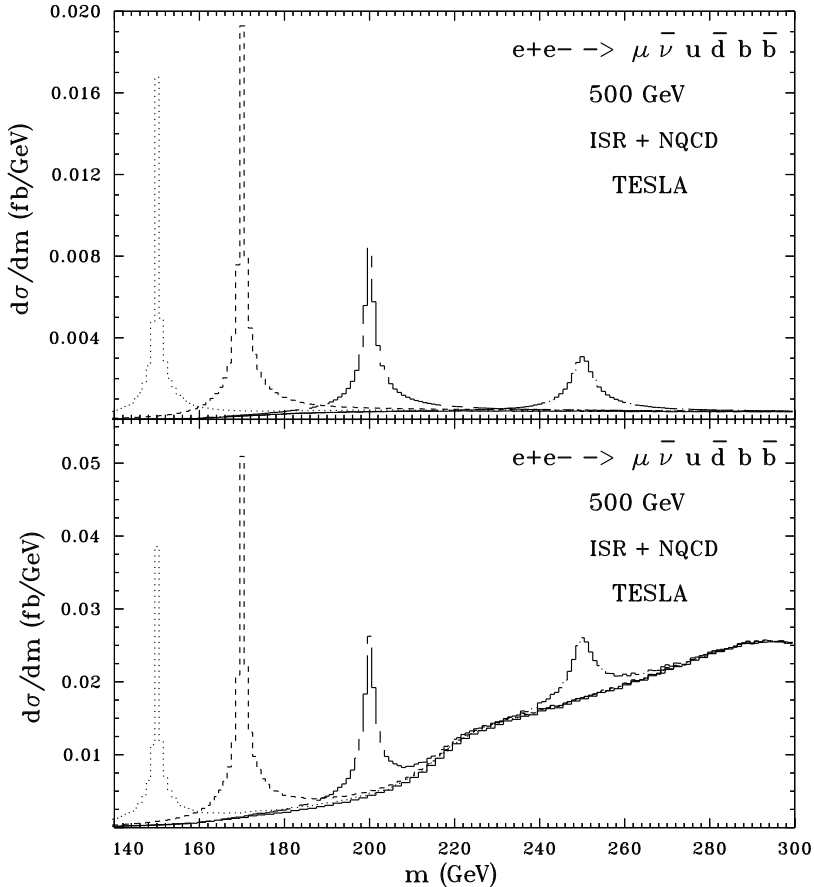


Figure 7: *Reconstructed mass distributions with normal cuts (lower) and normal cuts + $|M - m_{top}| > 40$ GeV ($M = m(bud\bar{b})$ and $m(b\bar{u}d\bar{b})$) (upper). The continuous line represents the total background. The others correspond to the total cross sections for (from left to right) $m_h = 150, 170, 200, 250$ GeV.*

2) and 3). The other type of signal events which can be studied with CC cross sections is $l \nu_l + l' \nu_{l'} + l'' \bar{l}''$ but it amounts only to .7% of the ZH events and will not be considered. All other events with two ν 's of the same flavour in the final state and/or with both W's decaying hadronically cannot be discussed without the full NC, MIX and CC contributions to the irreducible background.

The isolated lepton (e.g. a μ^- without the corresponding μ^+) characteristic of events 1), 2), 3) can be considered an experimental signature that in the process two W's have been produced. It is therefore extremely useful in reducing the background. On the other hand the neutrino makes the reconstruction of the Higgs mass more difficult, as missing energy and momentum are also due to ISR and BST.

The main six fermion background to events of type 1) comes from $t\bar{t}$. With b-tagging it can be greatly reduced when the 4 q's are light ones. In this case it is however more difficult to find out which pair of quarks pertains to the Z and which enters in H mass reconstruction. The signal events of type 1) with 2 b's are about 6.8% of the total HZ signal.

In order to properly understand $t\bar{t}$ background, we take as a case study the reaction

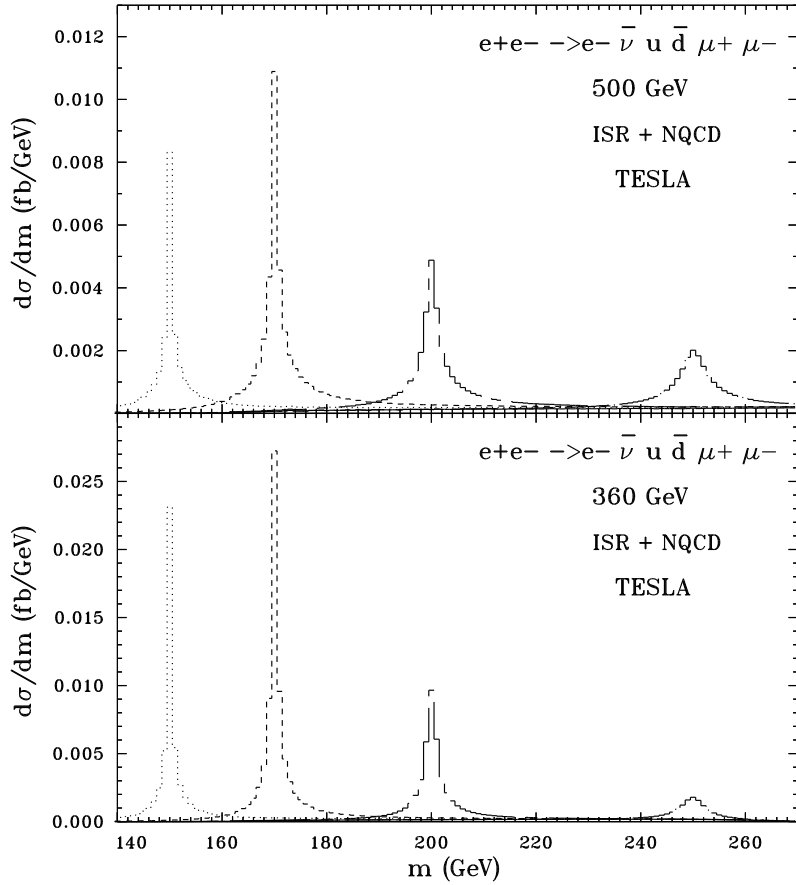


Figure 8: *Reconstructed* mass distributions with *normal* cuts . The continuous line represents the total background. The others correspond to the total cross sections for (from left to right) $m_h = 150, 170, 200, 250$ GeV.

$e^+e^- \rightarrow \mu\nu u\bar{d} b\bar{b}$. The most relevant distribution to analyze in Higgs physics is the invariant mass of the particles which in the signal diagram decay from the Higgs. This distribution is however not directly measurable when at least one of the W's decays leptonically. We will therefore consider two other distributions. We will call *reconstructed* the distribution in which all missing 3-momentum is attributed to the neutrino, and its energy is taken to be equal to its modulus. We will instead name *missing* the distribution of the invariant mass of the 4-momentum recoiling from the Z-decay particles ($P_{tot} - P_b - P_{\bar{b}}$ in the case at hand). In fig. 6 are reported the above distributions both for the signal ($m_h = 170$ GeV) and for the background. One notices an expected broadening of the peak for the *reconstructed* distribution. The *missing* distribution produces in addition a typical distortion of the signal and a shift of the background toward higher masses. For such a reason we will examine in the following *reconstructed* distributions, apart from processes of type 3) above, where only the *missing* one is measurable, due to the presence of two neutrinos whose 3-momentum cannot be separately reconstructed. Here and in the following we apply the request that the invariant mass of the two particles decaying from the Z and the two quarks eventually decaying from the W, be within 20 GeV from the Z and the W mass

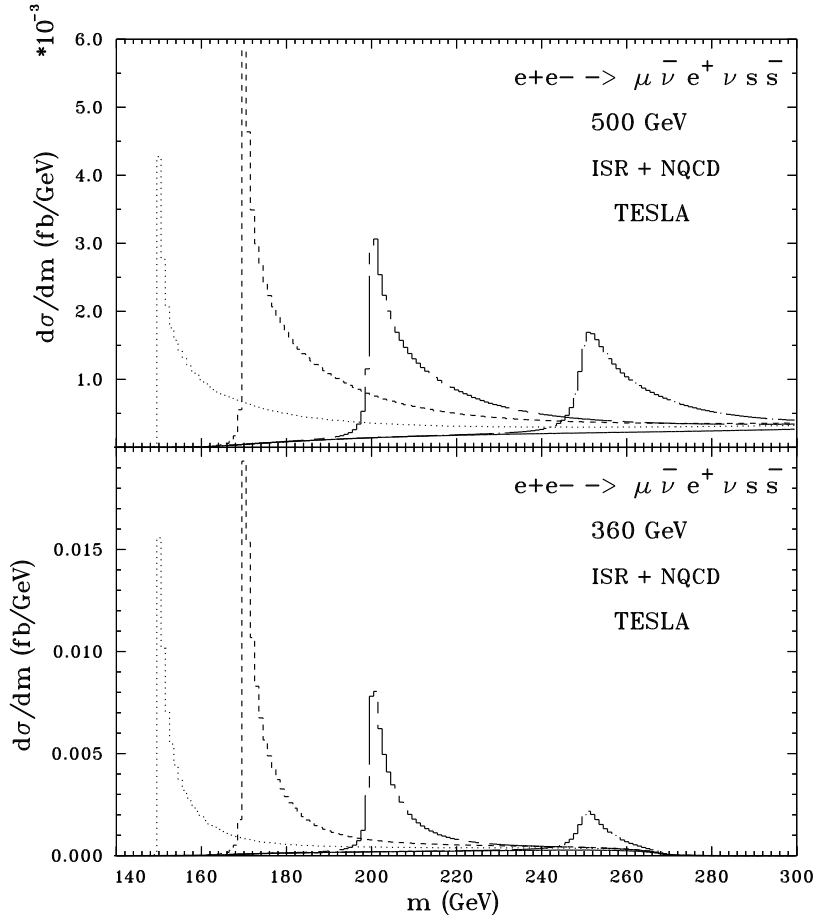


Figure 9: *Missing* mass distributions with *normal* cuts . The continuous line represents the total background. The others correspond to the total cross sections for (from left to right) $m_h = 150, 170, 200, 250$ GeV.

respectively. We refer to these cuts, in addition to those described in the introduction, as *normal* cuts. From fig. 7 (lower) one can realize that such cuts are already rather effective in reducing $t\bar{t}$ background, especially for low m_h values. One can try to reduce it further with the additional cuts $|m(bud\bar{d}) - m_{top}| > 40$ GeV and $|m(\bar{b}ud\bar{d}) - m_{top}| > 40$ GeV. The upper part of fig. 7 shows that in such a case the background becomes completely negligible, but at the price of reducing also the signal by an approximate factor 3.

In order to analyze intermediate Higgs production in the final states 2) and 3) we consider the processes $e^+e^- \rightarrow e\bar{\nu}u\bar{d}\mu^+\mu^-$ and $e^+e^- \rightarrow \mu\bar{\nu}_\mu e^+\nu_e s\bar{s}$ respectively. For the first of the two, fig 8 shows that with *normal* cuts and for the *reconstructed* mass the whole contribution of the hundreds of background diagrams is practically almost irrelevant both at 360 and 500 GeV center of mass energy. For most studies a reasonable approximation in such a case would be to consider only the off-shell six fermion signal diagram $e^+e^- \rightarrow H^*Z^* \rightarrow W^{*+}W^{-*}Z^* \rightarrow e\bar{\nu}u\bar{d}\mu^+\mu^-$. A similar conclusion (see fig. 9) applies also to $e^+e^- \rightarrow \mu\bar{\nu}_\mu e^+\nu_e s\bar{s}$ at 360 GeV. At 500 GeV the background becomes somewhat more important and the tail of the *missing* distribution can be exactly reproduced only with the full calculation.

5 Conclusions

Six fermion processes will become relevant at future e^+e^- linear colliders.

With the help of the helicity amplitude method of ref. [9][10], we have built up a program (SIXPHACT) to compute all complete tree level charged current cross sections. The program can also compute any differential cross section (distribution) with high precision in reasonable computer time. Complete six fermion calculations are in fact particularly useful when studying distributions, where one can understand the differences from the usual *production* \times *decay* approximation and analyze for instance which cuts have to be imposed to enhance signals with respect to irreducible backgrounds.

We have given some examples of phenomenological studies relevant to top, WWZ and Higgs physics. We have in particular found that single resonant background contributions are difficult to get rid of when studying invariant mass or angular top distributions. For WWZ it seems that *production* \times *decay* approximation is not viable, and that to get rid of the irreducible background with the cuts we have tried, one loses about 10% of events with a muon in the final state and more than 30% for an electron at 500 GeV. The enormous amount of background coming from $t\bar{t}$ production is under control when appropriate b-tagging and cuts are applied. For what concerns intermediate Higgs physics, we have restricted our analysis to final states with at least an isolated lepton which most probably comes from a W decay. The most important contribution to the signal comes from final states with four quarks. These events suffer from $t\bar{t}$ background which we have analyzed in detail and found to be greatly reduced by a simple cut on the invariant mass of the quarks decaying from Z. Processes of the type $l\nu_l + l'\bar{l}' + 2q's$ have a harmless irreducible background with a cut on $l\bar{l}$ invariant mass. Finally processes of the type $l\nu_l + l'\nu'_l + 2q's$ can also give an important contribution to Higgs studies if their *missing* mass distribution is carefully analyzed.

References

- [1] Physics at LEP2, G. Altarelli T. Sjostrand, F. Zwirner eds., CERN 96-01
- [2] D. Bardin, R. Kleiss et al., *Event Generators for WW Physics* in ref. [1];
M. L. Mangano, G. Ridolfi et al., *Event Generators for Discovery Physics* in ref. [1]
- [3] E. Accomando, A. Ballestrero, *Comp. Phys. Commun.* 99 (1997) 270.
- [4] D. Bardin, M. Bilenky, D. Lehner, A. Olchevski, T. Riemann, *Nucl. Phys. (Proc. Suppl.)* 37B (1994) 148;
- [5] E. Accomando, A. Ballestrero, M. Pizzio, *Torino Prep. DFTT* 74/96, hep-ph/9706201.
- [6] A. Ballestrero, E. Maina, S. Moretti, *Phys. Lett.* B333 (1994) 434
A. Ballestrero, E. Maina, S. Moretti, *Phys. Lett.* B335 (1994) 460.
- [7] G. Montagna, M. Moretti, O. Nicrosini, F. Piccinini, *Pavia Prep. FNT/T-97/10*, hep-ph/9705333.

- [8] F. Yuasa, Y. Kurihara, S. Kawabata, KEK Prep. 97-42, hep-ph/9706225.
- [9] A. Ballestrero, PHACT 1.0 - Program for Helicity Amplitudes Calculations with Tau matrices; Torino prep. in preparation.
- [10] A. Ballestrero, E. Maina, *Phys. Lett.* B350 (1995) 225.
- [11] E. A. Kuraev, V. S. Fadin, Sov. J. Nucl. Phys. **41** (1985) 466; G. Altarelli, G. Martinelli, in *Physics at LEP*, CERN 86-02, J. Ellis, R. Peccei eds. (CERN, Geneva 1986), vol I, pg. 47; O. Nicrosini, L. Trentadue, *Phys. Lett.* B196 (1987) 551.
- [12] T. Ohl, *Comp. Phys. Commun.* 101 (1997) 269.
- [13] G.P. Lepage, *Jour. Comp. Phys.* 27 (1978) 192.
- [14] J. Jersak, E. Laermann, P.M. Zerwas, *Phys. Rev.* D25 (1982) 363; J. Schwinger, 'Particles, Sources and Fields', Addison-Wesley (1973); L. Reinders, H. Rubinstein, S. Yazaki, *Phys. Reports* C127 (1985) 1.
- [15] F. Abe et al. (CDF Coll.), *Phys. Rev.* D50 (1994) 2966 and *Phys. Rev. Lett.* 74 (1995) 2626; S. Abachi et al (D0 Coll.), *Phys. Rev. Lett.* 74 (1995) 2632.
- [16] V.S. Fadin, V.A. Khoze, JETP Lett. 46 (1987) 525, Sov. J. Nucl. Phys. 48 (1988) 309; M.J. Strassler, M.E. Peskin, *Phys. Rev.* D43 (1991) 1500; M. Jezabek, J.H. Kühn, T. Teubner, *Z. Phys.* C56 (1992) 653; Y. Sumino, K. Fujii, K. Hagiwara, M. Murayama, C.K. Ng, *Phys. Rev.* D47 ((1992)) 56; M. Jezabek, J.H. Kühn *Phys. Lett.* B316 ((1993)) 360.
- [17] W. Bernreuther, O. Nachtmann, P. Overmann, T. Schröder, *Nucl. Phys.* B388 (1992) 53, B406 (1993) 516; G. L. Kane, G. A. Ladinsky, C. P. Yuan, *Phys. Rev.* D45 (1991) 124.
- [18] J. Kalinowsky *Acta Phys. Polon.* B23 (1992) 1237; G. Blanger, F. Boudjema, *Phys. Lett.* B288 (1992) 201; F. Boudjema, LAPP prep. ENSLAPP-A-431-93 (1993), hep-ph/9308343.
- [19] A. Miyamoto, Kek prep 95-185 (1995).
- [20] A. Dobado, M.J. Herrero, J.R. Pelaez, E. Ruiz Morales, M.T. Urdiales, *Phys. Lett.* B352 (1995) 400; A. Dobado, M.T. Urdiales, *Z. Phys.* C71 (1996) 659.